Magnetism in non-stoichiometric goethite of varying total water content and surface area

C. A. Barrero,[1] J. D. Betancur,[1] J. M. Greneche,[2] G. F. Goya[3] and T. S. Berquó[3]

[1]*Grupo de Estado Sólido, Instituto de Física, Universidad de Antioquia, A. A.* 1226 *Medellín, Colombia. E-mail: cbarrero@pegasus.udea.edu.co*

[2]*Laboratoire de Physique de l'Etat Condensé, UMR CNRS* 6087, *Université du Maine,* 72085 *Le Mans, Cedex* 9, *France*

[3]*Laboratorio de Materiais Magnéticos, Instituto de Física, Universidade de São Paulo, Brazil*

SUMMARY

In this work, the magnetic properties of four non-stoichiometric goethites with varying total water content and surface area have been investigated. The samples were prepared using two different hydrothermal methods, deriving either from Fe(II) precursors or from Fe(III) precursors. The effects of both agitation during mixing solutions and drying time during synthesis upon the physical properties of the final products were also studied. The samples were characterized by XRD, TGA, BET, [57]Fe Mössbauer spectrometry at 300 K, 77 K and 4.2 K, ZFC and FC curves, and magnetization curves. The goethites synthesized from the Fe(II) precursors result less crystalline, contain higher water content than those prepared from the Fe(III) precursor. In addition, ferrous precursor goethites exhibit superparamagnetic relaxation effects, while the ferric precursor goethites exhibit magnetic ordering of clusters. It is found that the stirring process during synthesis can affect the total water content and the magnetic behaviour of the goethites. Our results suggest that structural water content decreases the magnetic hyperfine field at 4.2 K. The adsorbed water content also affects this parameter as suggested by *in situ* annealing cycles of the goethites in a Mössbauer cryofurnace. Finally, we propose an unique 2-D phase diagram to describe all the magnetic properties of present goethites observed as a function of temperature, surface area (or particle size) and total water content.

Key words: crystallinity, goethite, magnetic properties, surface area, water content.

1 INTRODUCTION

Goethite (α-FeOOH) is a fascinating iron oxyhydroxide. Indeed, it is commonly found in natural ecosystems and is by far the most common iron oxyhydroxide in terrestrial soils, sediments and clays (Schwertmann & Cornell 1991; Cornell & Schwertmann 1996; De Grave *et al.* 2002; Guyodo *et al.* 2003). It was previously ignored in palaeomagnetic and rock magnetic studies until it was discovered that it could carry a stable remanence (Strangway *et al.* 1968; Hedley 1971; Dekkers 1989a,b). Since then, increasing efforts have been put forward in order to fully understand the physical origin of the complex magnetism exhibited by this sample. Goethite is generally thought to be the source of disturbing secondary magnetizations in sediments. This iron phase has been used to quantify variations in Aeolian dust inputs into oceans (Maher & Dennis 2001) and recently goethite has also been associated with investigations into the effect of dissimilarity metal reducing bacteria on sediment geochemistry (Cooper *et al.* 2005). This phase exhibits weak ferromagnetism (WFM) while other magnetic properties strongly depend on its structural and microstructural properties.

Goethite is one of the most important products of the atmospheric corrosion of iron and steel, which can drive them protective properties (Lee *et al.* 2001). Goethite is sometimes used as a starting material to produce maghemite, which is used as magnetic pigment (Nuñez *et al.* 2000). It can also be used as a ferrofluid, thanks to its interesting magnetic properties (Lemaire *et al.* 2002).

Previous investigations have demonstrated that the crystallographic and the magnetic unit cell of goethite have the same size (Forsyth *et al.* 1968), and that below the Néel temperature (about 400 K), the iron moments are collinear in a two sublattice antiferromagnetic (AFM) structure and lie parallel to the *c*-axis (space group Pbnm). However, other authors (Coey *et al.* 1995) have reported that goethite orders in a non-collinear four sublattice AFM structure, with a canting angle of $\pm 13°$ with respect to the *c*-axis. This value was obtained by refinements of the structural parameters and moment in spin modes on the powder neutron diffraction data of a natural fibrous goethite from Cary Mine, Ironwood, Michigan. The canting angle in this goethite is not related to a magnetic transition like the Morin transition in haematite, but it seems to be permanent and related to the presence of impurities and imperfections in the lattice of the sample.

Most of the natural and synthetic goethites exhibit rather poor crystallinity and rather small particle size. Their specific areas, for instance, may range from 8 to 200 m^2 g^{-1} (Schwertmann *et al.*

1985; Cornell & Schwertmann 1996). As a consequence they have a defective structure, which influences all their physical properties, especially the magnetic ones. First of all, they contain more water than the amount predicted by the theoretical formula. In order to account for this additional water content a general formula for goethite has been proposed, namely, $\alpha - (Fe)_{1-y/3} O_{1-y} (OH)_{1+y}$, in which $y/3$ represents the fraction of Fe replaced by $3 H^+$ (Schulze & Schwertmann 1984; Wolska & Schwertmann 1993). Secondly, many structural defects occur in the goethite crystals, such as point defects and intergrowths. Schulze & Schwertmann (1984) have found that the presence of structural defects makes the hydrogen bonds weaker, decreases the temperature of dehydroxylation, increases the amount of hydroxyl and water content, reduces the crystal size and increases the dissolution rate in acid.

Among the physical properties of goethite, the magnetic properties remain the most difficult to interpret. Indeed, various models have been put forward in order to account for the magnetic behaviour, but some models still remain controversial. The strongest magnetic interaction between nearest-neighbours Fe ions is AFM. In the simplest case, this results in the creation of two magnetic sublattices, both having the same temperature-dependent sublattice magnetization $M(T)$. To our knowledge, three types of theoretical models describing $M(T)$ have been at least put forward: all of them are expected to be valid over the entire temperature ranging from 0 K up to the transition temperature, the main difference between them being the mechanism involved in the magnetic ordering. The first model considers the magnetic ordering of spins (De Grave & Vandenberghe 1986; Van der Woude & Dekker 1966; Kilcoyne & Ritter 1997), the second considers the ordering of magnetic clusters (Bocquet *et al.* 1992; Bocquet & Kennedy 1992) while the third considers the ordering of interacting magnetic particles (Morup *et al.* 1983). In the cluster coupling model, the particles themselves may be considered as being made up of interacting magnetic clusters, with an ordering temperature of T_N, whereas in the particle coupling model the particles themselves as a whole interact with their neighbours. However, those models do not fully satisfy the magnetic properties of all the samples. As a rule of thumb, it seems that both the particle size and the degree of crystallinity are the main factors determining the type of mechanism involved in the magnetic ordering. Barrero *et al.* (1999) have tried to classify the magnetic behaviour of the goethites according to their particle sizes. In contrast, the degree of crystallinity in a sample is usually more difficult to quantify. On the other hand, the temperature dependence of the magnetization at the surface of nanoparticles has been found to be much steeper than that in the core. Yamamoto *et al.* (1993) have calculated this dependence using the Brillouin function assuming the surface spin being equal to 5/2 and the surface exchange field to be reduced with respect to the core exchange field.

In spite of the simplifying efforts, the actual experiments on the magnetic behaviour of goethites are even more complicated. For example, several authors have reported that natural and synthetic goethites possess a small net magnetic moment (Strangway *et al.* 1968; Hedley 1971; Broz *et al.* 1990; Coey *et al.* 1995; Özdemir & Dunlop 1996; Broz & Sedlak 1991; De Boer & Dekkers 1998; Guyodo *et al.* 2003). The WFM was found to be also parallel to the crystallographic *c*-axis, while the Curie point (T_C) was found to be equal to the Néel point (T_N) (Özdemir & Dunlop 1996). Other features like reduction and distribution of the transition temperatures and of the exchange interactions, as well as lowering of the saturation magnetization have been observed in these systems and explained on the basis of surface effects, structural defects or the presence of impurities (Murad 1996).

From this literature review, one concludes that the magnetic properties of α-FeOOH are strongly affected by both the particle size and the degree of crystallinity. However, most of the work has been related to the particle size, which is rather easy to measure. In contrast, the degree of crystallinity in a sample is usually more difficult to quantify. The usual way derives from the mean coherence length in a certain crystallographic direction, which is determined from the line broadening of the corresponding X-ray reflection. However, this term is very complex because it includes mixed contributions coming from small particle size and non-stoichiometry, which is essentially due to the presence of H_2O and/or OH^- bound into the structures. In this work, the degree of non-stoichiometry and the surface area will be related to the degree of crystallinity of the sample. To the best of our knowledge, there is a lack of work related to the effect of total water content on the magnetic properties of non-stoichiometric goethite: this is the main purpose of the present investigation. For completeness, the surface areas and grain sizes of the samples are also considered in this work.

2 EXPERIMENTAL PART

To obtain goethites with a broad range of water contents, four different samples were prepared according to literature procedures, but introducing small variations in some steps as follows. Two of them were precipitated from Fe(II) precursors according to the procedure described in Section 5.3. of Schwertmann & Cornell (1991). Aqueous solutions of $FeCl_2.4H_2O$ and $NaHCO_3$ were mixed under a constant flux of air and once the oxidation was completed, the product was filtrated, washed several times, and dried in an oven at 40 °C. The powdered samples dried for 24 hr and 48 hr were named GOE24H and GOE48H, respectively. The other two samples were prepared from Fe(III) precursors by mixing $Fe(NO_3)_3.9H_2O$ and KOH aqueous solutions following procedure 5.2.1. described in the reference above. The reaction after mixture took place at 70 °C for 60 hr. The samples were named GONOSA and GONITRA. During the reaction, for the first sample the mixture was left in repose inside the oven, whereas for the second case the mixture was constantly stirred with a magnetic bar encased in chemically inert Teflon. Finally, the products were filtrated, washed several times, and dried in an oven at 40 °C. According to Schwertmann and Cornell (1991), the particle shape of the goethites from Fe(III) precursors is acicular, and consist of several domains along the needle axis. Those goethites from Fe(II) precursors are of lower crystallinity and consist of agglomerated grains of acicular-like shapes.

All the powdered samples were characterized using several techniques. X-ray diffraction (XRD) measurements was performed on a BRUKER AKS D8 ADVANCE equipped with a PSD detector and a Co tube. The scans were done in the range of 10 °–80 °(2θ) at 0.014 ° per second. Thermogravimetric analysis (TGA) was done in a TA Instruments 2950 TGA HR V6.1A. The curves were obtained using about 15 mg of sample submitted to a flux of 100 mL min^{-1} of N_2 UAP and a heating rate of 10 °C min^{-1} from room temperature till 900 °C. BET analysis with N_2 was performed in a ASAP 2010 V4.00 D. All induced magnetization measurements were performed by using a commercial SQUID magnetometer (MPMS—Quantum Design). Zero-field-cooled (ZFC) magnetization curves were obtained by cooling in zero field from a high temperature (300 K) to a low temperature and then measuring the magnetization at stepwise increasing temperatures, from 2 K to 400 K, in a small applied field ($B = 50$ mT). The sample was again cooled, in the same field, and field cooled (FC) magnetization curves were obtained by measuring
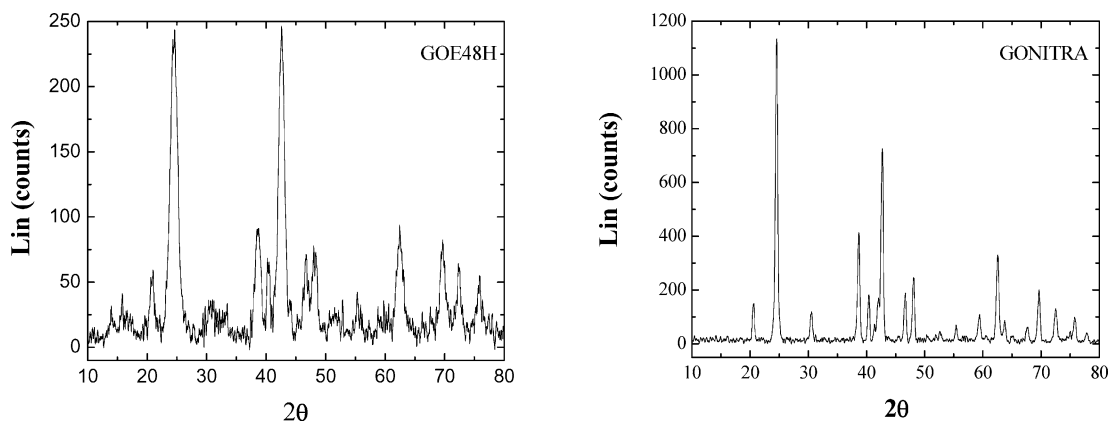
Figure 1. X-ray diffractograms for some selected samples.

at stepwise increasing temperatures. An additional induced magnetization curve was obtained by cooling the sample in a field of 1 T and measuring in the same field at stepwise increasing temperature up to 400 K. Mössbauer spectrometry at 300 K, 77 K and 4.2 K were obtained in a conventional spectrometer working in the transmission mode, with a constant acceleration drive using a 25 mCi Co^{57}/Rh source and a cryofurnace (77–680 K) to perform temperature and *in situ* temperature cycling measurements. Analysis of the spectra was performed by using least-square fitting programs. Quadrupolar doublets and magnetic sextets composed of Lorentzian lines were considered. The isomer shift values are quoted to that of α–Fe at 300 K.

Mössbauer spectrometry was also used to perform several *in situ* annealing cycles applied to some samples with the purpose of removing the adsorbed water content. For GOE48H, in the first cycle, the sample was heated for 30 min at 380 K, below the temperature of the phase transition into haematite. Afterwards, the sample was cooled down inside the cryofurnace to 77 K to get *in situ* Mössbauer spectrum (MS). In a second cycle, the temperature was raised again to 370 K for 90 min and lately the MS was collected again at 77 K. For GONOSA and GONITRA, several cycles at 365 K, 370 K, 375 K and 380 K for 30 min were performed and each corresponding MS was recorded *in situ* at 77 K. Finally, MS were collected at 77 K after removing each sample from the cryofurnace and then exposed to the open atmosphere, in order to check the possible reabsorption of water.

3 RESULTS AND DISCUSSION

3.1 Structural characterization

Typical X-ray diffractograms for some selected samples are shown in Fig. 1. As expected (Schwertmann & Cornell 1991), XRD patterns of the goethites prepared from Fe(III) precursors consist of Bragg peaks that are only assigned to goethite, allowing us to conclude

to a rather good purity. This result is in good agreement with the 77 K MS (see below), which showed sextets with hyperfine fields larger than 49.6 T assigned only to goethite, whereas the presence of magnetically ordered lepidocrocite (at 77 K) is rejected here because there is no sextet with a hyperfine field of about 45.8 T. In the case of sample GOE48H, one observes in addition to peaks clearly attributed to goethite, another small peak located at about 17 °, which is assigned to the lepidocrocite phase. The formation of this phase might be related to a larger than expected rate of oxidation. In spite of this, we are assuming that the presence of lepidocrocite in the goethites prepared from Fe(II) precursors does not affect noticeably the interpretation of final results, because of its minor relative amount (less than ∼10 weight per cent). As we will see later, room temperature and 77 K MS support this idea. Fig. 1 reveals that the Bragg peaks for sample GOE48H are broader than those of GONITRA: this broadening has to be attributed to both the poor degree of crystallinity and the lower crystalline grain size of the samples prepared from the Fe(II) precursors in comparison to those prepared from Fe(III). In fact, this is reflected in the different average grain sizes of the samples as determined from the X-ray patterns (see Table 1).

BET surface area values for all the samples are also listed in Table 1. It is possible to notice that the goethites prepared from Fe(II) precursors exhibit larger surface areas in comparison to the goethites prepared from Fe(III) precursors. These results are consistent with XRD data. In the case of Fe(III) goethites, the lower surface area of GONITRA in comparison to that of GONOSA may suggest that the stirring process during synthesis can affect the surface area and the particle size of the final product, thus producing slightly larger goethites.

The structural hydroxyl and adsorbed water contents were determined from the TGA curves (see Fig. 2 and Table 1). Each curve shows essentially two regions of weight loss, which were evidenced from the first derivative of the TGA curves, the first one occurring at about 341 K, 341 K, 326 K and 321 K, for samples

Table 1. Adsorbed (per cent H$_2$O), structural (per cent OH) and total (per cent ΔOH) water content, as well as values for the non-stoichiometric parameter (*y*) and surface area (*S*) for all samples, and Néel (T_N) and blocking temperatures (T_B). The numbers in parenthesis indicate the uncertainty in the last digit.

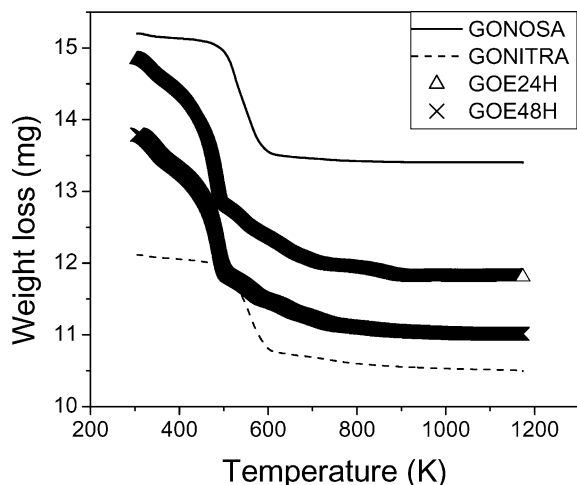| Sample	Per cent H$_2$O	Per cent OH	Per cent ΔOH	y	S (m^2 g^{-1})	(Per cent ΔOH)/S	Grain size (nm)	T_N (K)	T_B (K)
GOE24H	0.97(3)	19.4(1)	20.4(1)	0.76(1)	135.6(4)	0.15		310(2)	279(2)
GOE48H	1.36(3)	18.7(1)	20.1(1)	0.63(1)	153.4(4)	0.13	6	310(2)	262(2)
GONITRA	0.11(3)	13.4(1)	13.3(1)	0.25(1)	27.8(1)	0.48	24	387(2)	—
GONOSA	0.10(3)	11.8(1)	11.7(1)	0.13(1)	32.5(2)	0.36	17	387(2)	—

Figure 2. Thermogravimetric curves for all samples.

GOE24H, GOE48H, GONITRA, and GONOSA, respectively. This phenomenon is mainly assigned to the departure of surface water (per cent H_2O) (Schwertmann *et al.* 1985; Özdemir & Dunlop 2000). The second and most important region of weight loss, which is associated to the departure of structural hydroxyl (per cent OH), is relatively more abrupt for the Fe(III) goethites than for the Fe(II) goethites. For the first two samples, it ends at about 700 K, whereas for the others, it finishes at about 900 K. Above this temperature the weight remains rather constant. The shape of these curves could be related to the lower degree of crystallinity of the goethites from Fe(II) precursors in comparison to the goethites from Fe(III) precursors (Schwertmann & Cornell 1991).

The chemical formula for non-stoichiometric goethite is given by α-$Fe_{1-(y/3)}O_{1-y}(OH)_{1+y}$, where y represents the non-stoichiometric parameter. The per cent OH can be related to the hydroxyl content in the goethite's formula through the following equation (Schulze & Schwertmann 1984; Wolska & Schwertmann 1993):

per cent OH $= [93.56(1 + y)/9.24 - 1.83y]$.   (1)

On the other hand, the total water content (per cent ΔOH) is given

by:

per cent $\Delta OH =$ per cent OH + per cent H_2O.   (2)

From the calculated data listed in Table 1, one can conclude that goethites prepared from the Fe(II) precursors contain more structural (and thus more vacancies) and surface water and hence more total water molecules than goethites prepared from the Fe(III) precursors. Additionally, the present results suggest that the stirring process during synthesis may improve the incorporation of OH groups into the goethite structure. Indeed, the agitation of the mixture of reactants makes probably the solution more homogeneous and thus favours a much more effective incorporation of the ions into the crystalline structure.

3.2 Magnetic characterization

Fig. 3 shows the ZFC/FC induced magnetization curves for each one of the samples. One observes that the FC values are higher than the ZFC ones, suggesting a small net moment in the samples, the origin of which will be discussed later. On the other hand, the shapes of the curves and the magnetization are similar for the two goethites obtained from Fe(II) precursors (Figs 3a and b). For samples GOE24H and GOE48H (Figs 3a and b), there are different temperatures at which the ZFC branches present a bending upwards. Since the Néel temperatures, T_N, are above room temperature (see discussion below), these maxima can be associated to the blocking process of small magnetic clusters, thus determining the onset of superparamagnetic (SPM) behaviour, according to the small grain sizes. The blocking temperatures, T_B, estimated as the maximum of these peaks, were located at 279 and 262 ± 2K for GOE24H and GOE48H, respectively.

In contrast, the shapes of the curves for goethites from Fe(III) precursors are different from each other and from the previous ones. In the case of GONITRA, the ZFC and FC curves do not practically show irreversibility (see Fig. 3c). Such a behaviour is consistent with the 300 K MS, a well-resolved sextet. Both features indicate that static magnetic ordering prevails the SPM relaxation phenomena, because the clusters exhibit a larger size than those of previous case. Here, it is worth mentioning that Barrero *et al.* (1999) have adequately fitted the temperature dependence of the average
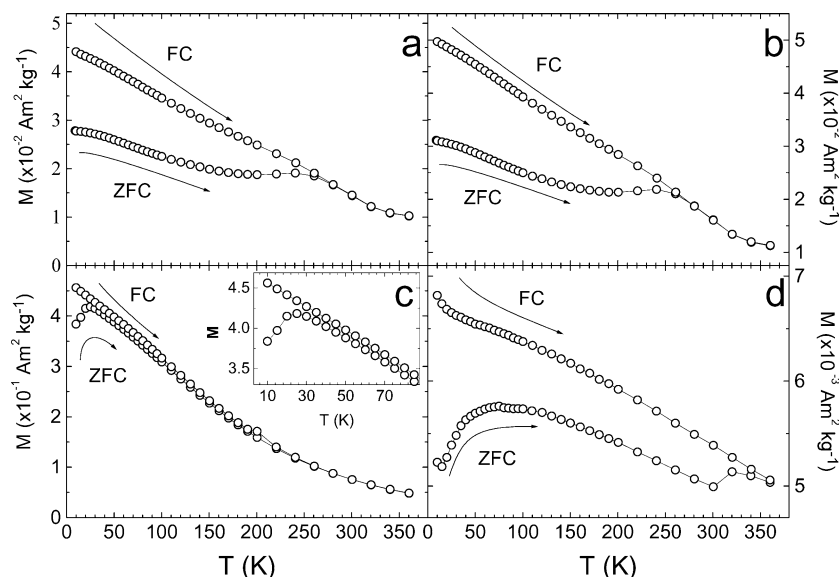

Figure 3. Induced magnetization curves (ZFC/FC) a field of 3.9 kA/<u>m</u> for samples: (a) GOE24H, (b) GOE48H, (c) GONITRA and (d) GONOSA.

magnetic hyperfine field with this model. One also observes that the ZFC curve exhibits a relatively sharp peak at around 30 K, which may be associated to a cluster glass ordering below this temperature. On the contrary, the FC/ZFC curves for GONOSA start to separate above 360 K, while the low-temperature sharp peak is found to be much broader (see Fig. 3d) . This broadening could be related to the fact that the temperatures for both cluster glass ordering and magnetic ordering of clusters are closer for GONOSA than for GONITRA.

The induced magnetization *M* scales of Figs 3(a) and (b) for samples from Fe(II) precursors are very similar. In contrast, the *M* scale for GONITRA is at least two and four orders of magnitude larger than those for GONOSA and the goethites from Fe(II) precursors, respectively. This behaviour for the Fe(II) goethites could be ascribed to a strong surface effects, which do not allow preferred magnetic orientation of the iron ions located at these sites. Indeed, the average net contribution of the grain boundaries to the total magnetization is very small while that of the crystalline grains is also very small due to the dominant AFM character. On the other hand, the large *M* values found for GONITRA in comparison to those for GONOSA, probably originate from larger amount of antiferromagnetically uncompensated sites in each magnetic cluster. This explanation is in agreement with the larger OH content and thus more vacancies are observed for GONITRA. Another possible explanation could come from different average cluster sizes.

Finally, the relative separation of the ZFC curve with respect to the FC one is larger for GONITRA than for GONOSA. This phenomenon could be related to different degrees of intercluster coupling, larger in the case GONITRA. In fact, it is expected that the higher the average magnetization per cluster, the larger would be the intercluster interaction.

Fig. 4 shows the induced magnetization curves for all samples, obtained under an applied field of 1 T. This field is enough to overcome any SPM fluctuations, and thus it is expected that any variation in the curve is due to intrinsic properties of the material close to the Néel point. It is possible to see that the shapes of the magnetization *versus* temperature (*T*) curves are similar for the goethites from Fe(II) precursors. The insert in Fig. 4 shows dM/dT *versus T* curves from which the minimum observed at about 310 K could be associated to the Néel temperatures (T_N) for both samples. The large reduction in T_N value or these samples as compared to that reported for well-crystallized large-particle goethite of
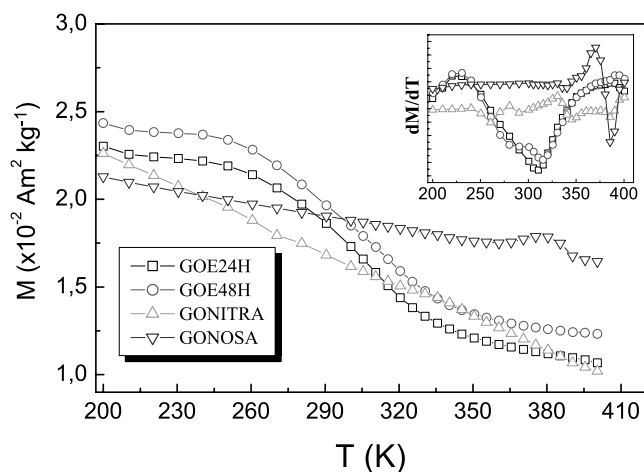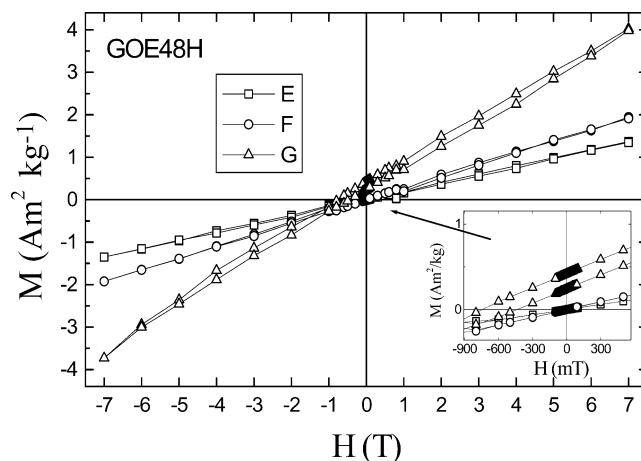

Figure 5. Hysteresis loops for GOE48H at different temperatures. All the loops were obtained after cooling in a 7 T field.

about 400 K, is due to mutual contributions coming from low crystallinity, high surface area, high concentration of defects, and large total water content. On the other hand, GONITRA and GONOSA have a T_N of about 387 K, evidencing better crystallinity and larger grain sizes of these samples as compared to the others. The T_N perhaps coincides with the onset of magnetic ordering of clusters. Another interesting behaviour could be seen in the magnetization curve for GONOSA: the magnetization goes through a maximum just below T_N, suggesting a Hopkinson effect. This pronounced peak is not clearly observed in the curve of GONITRA, perhaps implying that the agitation process during synthesis drastically affects the magnetic properties of the final product. This peak has also been observed in some natural and synthetic goethites (Hedley 1971; Broz & Sedlak 1991), but its origin is not yet clearly understood, to our knowledge. For single domain particles, this maximum can be due to the different temperature dependencies of the magnetization and anisotropy. There is no agreement in the literature as to whether the spontaneous magnetization is based on coherent rotation in a single domain particle or in the clusters, or even if the rotation is not coherent.

Fig. 5 shows the hysteresis loops for GOE48H at different temperatures. The magnetization of this sample is proportional to the applied field at 300 K and 400 K, suggesting a paramagnetic (PM) behaviour. Moreover, the loops show that the magnetization is not saturated at 7 T, as is reported by Rochette & Fillion (1989), and exhibits a extremely low coercive field, in contrary to that at 10 K. In addition, the centre of the loop is shifted towards negative fields by an amount of $H_e = \sim 0.6$ T (see the insert in Fig. 5), which can be due to the existence of an exchange bias between the weak ferromagnetic and AFM phases, which are present in this defective goethite. Let us remember that the WFM in goethite, which has been widely discussed in the literature, has been shown to be oriented parallel to crystallographic *c*-axis. Thermoremanence experiments (TRM) performed on oriented crystals of goethite clearly showed that the WFM of goethite is parallel to the AFM spin axis, which is also the *c*-axis (Figs 3 and 4 of Özdemir & Dunlop 1996). Various explanations of its origin have been reported. Moreover, it is well established that the balance of exchange interactions is modified at the surface because of missing iron neighbours. Néel (1962) has suggested that for small irregular particles containing *n* moments, the number of unbalanced spins is $n^{1/2}$. Thus, the average particle moment is given by $m(n^{1/2})$, where *m* is the average

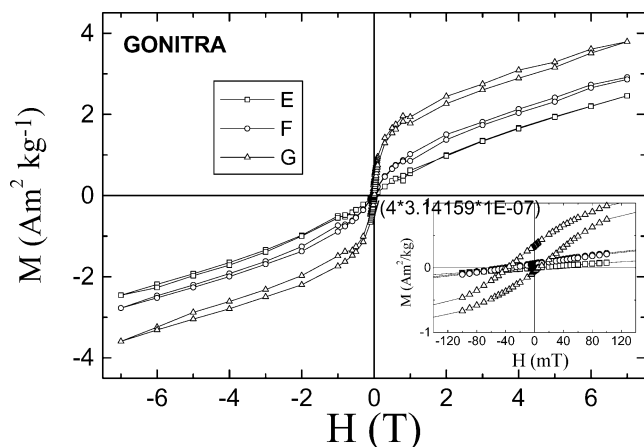**Figure 4.** Temperature dependence of the induced magnetization for all samples.

Figure 6. Hysteresis loops for GONITRA at different temperatures. All the loops were obtained after cooling in a 7 T field.

moment per iron atom. This model was applied by Strangway *et al.* (1968) to explain the thermoremanence magnetization observed in natural goethites when cooling in the presence of an external field. According to Broz *et al.* 1990; 1991), the net moment may also arise from the presence of unpaired chains at the surface. On the other hand, an iron neighbour can also be lost due to the presence of impurities, vacancies, and structural defects. In the case of the aluminium impurities, Hedley (1971) and Pollard *et al.* (1991) suggested that these ions may be preferentially located in one of the two magnetic sublattices, thus producing uncompensated spins. Finally, Coey *et al.* (1995) proposed that the origin of the small net moment may also originate from a hydrogen order. We conclude that the considerable amount of vacancies, and of structural defects, and the high surface areas are the main causes of the net moment in present Fe(II) goethites.

Fig. 6 shows the hysteresis loops for GONITRA at different temperatures. The shape of the loop at 300 K suggests a ferromagnetic-like behaviour in comparison to that at 400 K, but the ferromagnetism is more evident at 10 K. The hysteresis loops also show that the magnetization is not saturated at 7 T. The exchange bias is also observed (see inset in Fig. 6) ($H_e \sim 0.017$ T and $H_c \sim 0.02$ T), but its magnitude is lower than that for GOE48H. This behaviour supports the idea of better crystallinity for GONITRA than for GONOSA.

3.3 Mössbauer characterization

Room temperature MS for the goethites prepared from Fe(II) precursors consist of a doublet. In contrast, both room temperature MS of GONITRA and GONOSA consist of broadened lines, which can be described by means of a distribution of sextets. The refined values of the hyperfine parameters are listed in Table 2. At 4.2 K,

all samples are magnetically ordered. The MS and the derived hyperfine parameters at this latter temperature are reported elsewhere (Betancur *et al.* 2004).

We have performed multiple linear regression analysis between the water content and the hyperfine field at 4.2 K $B_{hf}(4.2$ K). It is found that the variations of this parameter are poorly described when only one of the structural properties is taken into account. For example, the linear correlation coefficients between B_{hf} and per cent H_2O is 0.12; between B_{hf} and S is 0.70, between B_{hf} and per cent ΔOH is 0.87, and between B_{hf} and parameter y is 0.62, etc. However, the linear correlation is noticeably improved when two physical properties are taken into account. The equation with the best correlation coefficient, where both parameter y and surface area S are considered, is expressed as:

$$B_{hf}(4.2K) = 50.8 - 0.6433y - 0.0023S \ (n = 13, \ R^2 \approx 0.91),$$
(3)

in which n is the number of data points, and R^2 is the linear correlation coefficient. In order to calculate this equation we have considered the data reported by Schwertmann *et al.* (1985). It is worth mentioning that they did neither report equation similar to those presented here, nor calculate the y values. Quantities y and S are commonly referred to as the degree of crystallinity. It is reasonable to assume that the effect of surface water content on $B_{hf}(4.2$ K) is reflected by the surface area, because both are directly correlated, that is, the larger the surface, the higher the surface water content is.

As expected, $B_{hf}(4.2$ K) decreases with increasing water content, mainly the structural water content. Indeed, the replacement of the Fe ions (magnetic ions) by hydroxyl groups (non-magnetic ions) and hence the presence of more vacancies (Schulze & Schwertmann 1984; Wolska & Schwertmann 1993), weaken the magnetic interactions. It is evident that both surface water and hydroxyl excess have some influence on the lattice parameters and consequently play a substantial role in the magnitude of the hyperfine field. Of course, these additional structural parameters are mainly determined by goethite formation factors such as crystallization, rates, temperature, etc.

The water content was also followed by performing several *in situ* annealing treatments to the samples inside the cryofurnace. Fig. 7 compares the spectrum at 77 K of GOE48H before and after a first annealing at 380 K for 30 min. One observes that the lines of the spectrum become more asymmetrically broadened after the treatment, and that the splitting between the first and sixth lines is reduced. This is reflected in the reduction by 9 T of the average hyperfine field $\langle B_{hf} \rangle$ (from 47.1 T before treatment to 38.1 T after treatment) (see Table 3). After the second annealing for 90 min at 370 K, a reduction is again noticed but rather small (1.1 T). Those experiments allow to conclude that most of the water is evaporated during the first cycle. In addition, the results for GOE24H are very similar.

Table 2. Hyperfine parameters obtained from the room temperature Mössbauer spectra for all samples. Estimated errors are about 0.1 T for $\langle B_{hf} \rangle$; and 0.01 mm s^{-1} for δ, Δ, 2ε, and $\tilde{\Gamma}$.

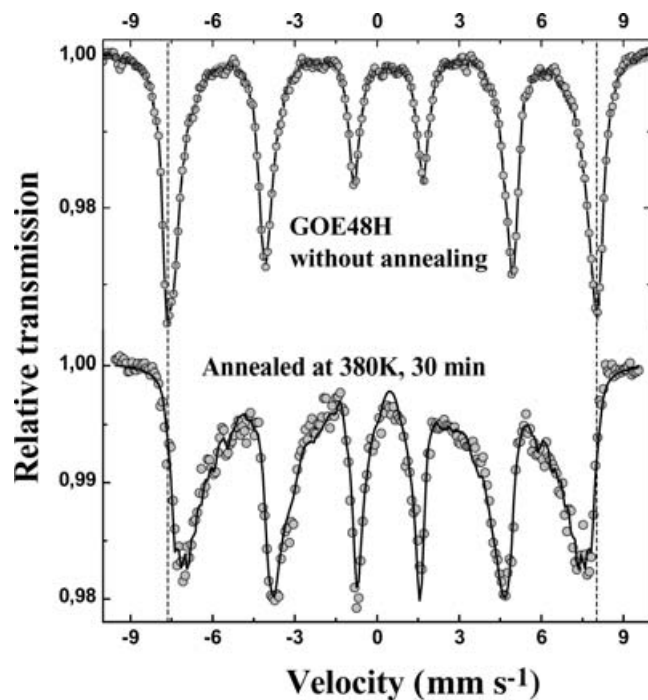| Sample | *Doublet component* | | | *Sextet component* | | | | Area |
	δ (mm s^{-1})	Δ	Γ	$\langle B_{hf} \rangle$	δ	2ε	Γ	
		(mm s^{-1})	(mm s^{-1})	(T)	(mm s^{-1})	(mm s^{-1})	(per cent)	
GOE24H	0.36	0.58	0.44	—	—	—	—	100
GOE48H	0.36	0.58	0.47	—	—	—	—	100
GONITRA	—	—	—	37.4	0.36	—0.25	0.26	94
GONOSA	—	—	—	37.0	0.37	—0.27	0.23	100

Figure 7. *In situ* Mössbauer spectra at 77 K for sample GOE48H before and after annealing processes.

Table 3. Hyperfine parameters at 77 K for samples before and after the annealing and rehydration treatments.

Sample	δ (mm s^{-1})	2ε (mm s^{-1})	$\langle B_{hf}\rangle$ (T)
Hyperfine parameters before annealing treatments			
GOE48H	0.47	−0.24	47.1
GONITRA	0.49	−0.28	49.8
GONOSA	0.46	−0.23	49.6
Hyperfine parameters after annealing treatments			
GOE48H[1]	0.47	−0.21	38.1
GOE48H[2]	0.47	−0.20	37.0
GONITRA[3]	0.44	−0.23	44.3
GONOSA[4]	0.47	−0.22	48.8
GONOSA[5]	0.47	−0.23	48.3
Hyperfine parameters after rehydration			
GOE48H	0.49	−0.23	45.2

1: First cycle at 380 K for 30 min; 2: Second cycle at 380 K for 90 min; 3: First cycle at 380 K for 90 min; 4: first cycle at 380 K for 90 min; 5: second cycle at 380 K for 90 min.

Fig. 8 compares the MS at 77 K of GONITRA before and after an annealing at 370 K for 60 min. The lines become more asymmetrically broadened after the treatment, however, in a lesser extent in comparison to GOE48H. The reduction for GONITRA of its $\langle B_{hf}\rangle$ at 77 K is about 5.5 T, whereas for GONOSA this change is only about 0.8 T (see Table 3). From Table 1, one concludes that the total water content of GONOSA is less than that for GONITRA, as reflected by the reduction of the hyperfine field. Again, there is an evidence that the magnetic stirring during synthesis affects the physical properties of the products. No appreciable changes in the hyperfine parameters were observed during the second annealing treatment for both samples. These latter results contrast with those obtained on GOE48H for which $\langle B_{hf}\rangle$ progressively decreases after each cycle.
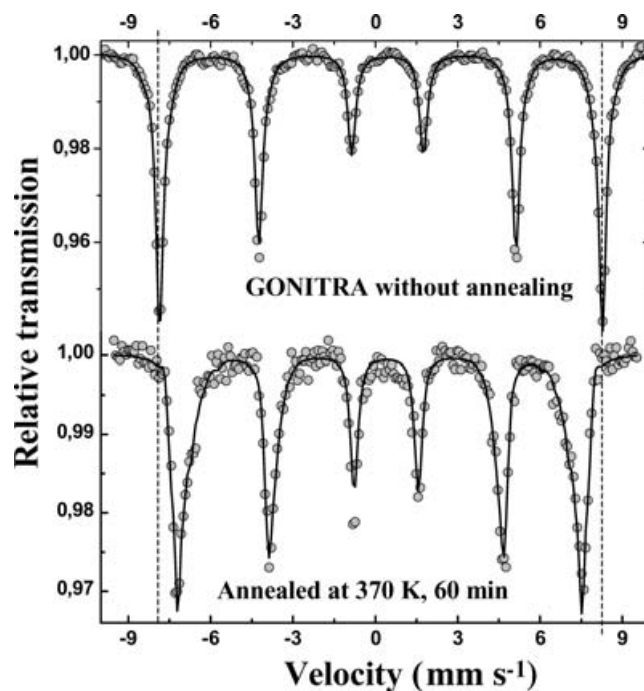
Figure 8. *In situ* Mössbauer spectra at 77 K for sample GONITRA before and after annealing processes.

At first, we tried to correlate all these data by means of a multiple linear regression analysis between the average reduced hyperfine field at 77 K, $\langle B_{r,77K}\rangle$, as defined below on one hand, and either per cent OH, per cent ΔOH, per cent H_2O or per cent ΔOH/S on the other hand. $\langle B_{r,77K}\rangle$ is defined as the difference between the average hyperfine fields obtained from the 77 K MS for the untreated sample, $\langle B_{r,\text{untreated}}\rangle$, and the sample after the first cycle, $\langle B_{r,\text{first−cycle}}\rangle$, with respect to the first one, according to the following equation:

$$\langle B_{r,77K}\rangle = \frac{\langle B_{\text{hf,untreated}}\rangle - \langle B_{\text{hf,first−cycle}}\rangle}{\langle B_{\text{hf,untreated}}\rangle}. \tag{4}$$

The reason to propose eq. 4 is that it takes into account a reference value, $\langle B_{r,\text{untreated}}\rangle$, which is the average hyperfine of the sample without any thermal treatment. In other words, $\langle B_{r,77K}\rangle$ is a weighted or ponderated value referred to $\langle B_{r,\text{untreated}}\rangle$. The best linear correlation coefficients R^2 are obtained for $\langle B_{r,77K}\rangle$ versus per cent OH ($R^2 = 0.94$) and for $\langle B_{r,77K}\rangle$ versus per cent ΔOH ($R^2 = 0.93$).

We also tried exponential relationships between $\langle B_{r,77K}\rangle$ and per cent OH, and also between $\langle B_{r,77K}\rangle$ and per cent ΔOH, which lead to correlation coefficients of $R^2 = 1$. Nevertheless, because of the low number of data points, it is difficult to decide which of the two relations, is the correct one. However, the linear and exponential relations suggest that the reduction in the hyperfine field is as large as the total water content is high. Indeed, we can expect that at the temperatures of annealing only adsorbed water content, that is, per cent H_2O, should be released. However, the correlation coefficients (for the exponential as well as the linear equations) are much better for per cent OH than for per cent H_2O.

Two possible mechanisms can be thus put forward. The first one considers the rupture of some goethite particles into a broad distribution of lower particle sizes because of the water pressure. Such an explanation is consistent with the reduction in the average hyperfine field and the asymmetrical broadening of the lines. A second scenario consists in the replacement of the water molecules and of some

hydroxyl groups by vacancy sites. According to the TGA results, at the annealing temperature, most of absorbed water is expected to be evaporated, while some hydroxyl groups can be also ejected, particularly for the Fe(II) goethites. More specifically, the temperature for the departure of adsorbed water occurs in the range of about 330 ± 10 K for all samples. Average weight loss values of 0.37 ± 0.03 per cent , 0.39 ± 0.04 per cent , 2.0 ± 0.2 per cent and 2.7 ± 0.3 per cent for GONOSA, GONITRA, GOE24H and GOE48H, respectively, are obtained in the temperature range from 365 K to 380 K. Thus, the goethites with large surface areas are expected to possess proportionally an high water content. In the case of Fe(III) goethites, the evaporated water could escape not only from the particle surface but also from the cluster frontiers. During the thermal treatment, a part of the water is evaporated, allowing a release of the hydroxyl and/or water groups, provoking thus the creation of vacancies. Because the interaction between the magnetic iron ions in goethite is mediated by these groups, a decrease of the magnetic interaction is expected, when they are released. This second hypothesis seems to be more realistic: indeed, after removing the sample from the cryofurnace and exposing to room atmosphere for a few hours, a MS was recorded at 77 K is again collected. As listed in Table 3, the hyperfine parameters of the untreated sample are almost recovered, in agreement with a rehydration of the samples.

3.4 Magnetic phase diagram for goethite

As mentioned earlier, Barrero *et al.* (1999) have made an attempt to classify the magnetic behaviour of goethite but only as a function of particle size (and hence surface area). However, the magnetic properties observed in goethite are much more complex and depend on more structural and chemical properties. Thus, we have attempted to incorporate in a unique phase diagram all the magnetic behaviours observed as a function of temperature, T, surface area, S (or particle size) and total water content, ΔOH. ΔOH takes into account the non-stoichiometric parameter y and the adsorbed water content, as given by eqs (1) and (2). A new schematic magnetic phase diagram is thus proposed in Fig. 9. Ideal goethite (ΔOH/S values above
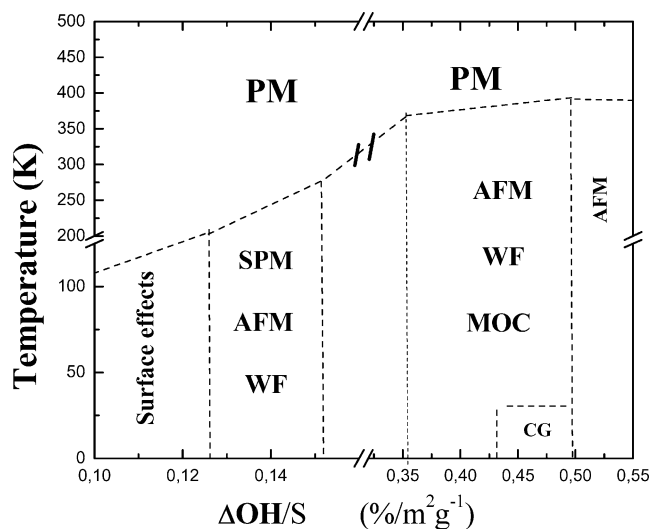
~ 0.50 per cent/m^2 g^{-1}), which has never been reported, with low S (or large particle goethite) and stoichiometric, that is, $y = 0$, below and above T_N is AFM and PM, respectively. As ΔOH/S decreases, and below T_N, goethite exhibits AFM, WFM and magnetic ordering of clusters (MOC). Above T_N, goethite is PM. It is interesting to mention that for certain ΔOH values and below certain temperatures (e.g. 30 K), goethite can exhibit cluster glass-like ordering (CG). As ΔOH/S decreases further, there are certain critical values, which strongly depend on particle size (surface area), for which goethite becomes SPM. Above certain S values, the magnetic properties are related to surface area properties. Of course, a precise line separating the different regions remains difficult to establish, but the present diagram shows some tendency (see the dotted lines in Fig. 9). It is important to emphasize that further investigations are needed to better characterize these regions.

4 CONCLUSIONS

We have studied the effect of the total water content and the surface area on the magnetic hyperfine properties of several non-stoichiometric goethites. It is found that these properties strongly depend on the synthesis conditions. Our results support the magnetic cluster ordering and SPM models depending upon the surface area and thus on the crystalline domain sizes. We also found that the drying time after the chemical reaction of the solutions does not appreciably affect the magnetic properties of the final products prepared from Fe(II) precursors. In contrast, the agitation during the mixture of the solutions in the goethites from Fe(III) precursors, provides significant effects on the properties of the products. In this case, more structural and adsorbed water content, slightly low surface area, cluster glass like with perhaps low magnetic coupling, and the lack of Hopkinson effect are some interesting characteristics of these goethites. We have proposed and explained two phenomenological equations, one linear and the other exponential, which relate the effect of water and/or hydroxyl contents on the average magnetic hyperfine field at low temperatures.

REFERENCES

Barrero, C.A., Vandenberghe, R.E. & De Grave, E., 1999. The effect of Al-content and crystallinity on the magnetic properties of goethites, *Hyp. Interactions,* **122,** 39–46.

Betancur, J.D., Barrero, C.A., Greneche, J.M. & Goya, G.F., 2004. The effect of water content on the magnetic and structural properties of goethite, *J. Alloys and Compounds,* **369,** 247–251.

Bocquet, S. & Kennedy, S.J., 1992. The Néel temperature of fine particle goethite, *J. Magn. Magn. Mat.* **109,** 260–264.

Bocquet, S., Pollard, R.J. & Cashion, J.D., 1992. Dynamic magnetic phenomena in fine-particle goethite, *Phys. Rev. B,* **46,** 11657–11644.

Broz, D. & Sedlak, B., 1991. Surface ferrimagnetism of synthetic goethite, *J. Magn. Magn. Mat.,* **102,** 103–108.

Broz, D., Reiman, S.I. & Sedlak, B., 1990. Mössbauer study of defective goethite, *Hyp. Interactions,* **60,** 1011–1014.

Figure 9. Schematic magnetic phase diagram for goethite as a function of the ratio $\frac{\text{per cent}\Delta OH}{S}$ of the total water content to the surface area. PM: paramagnetic, AFM: antiferromagnetic, WF: weakly ferromagnetic, SPM: superparamagnetic, MOC: magnetic ordering of clusters. CG: cluster glass-like order.

Coey, J.M.D., Barry, A., Brotto, J., Rakoto, H., Brennan, S., Mussel, W.N., Collomb, A. & Fruchart, D., 1995. *J. Phys.: Condens. Matter,* **7,** 759–768.

Cooper, D.C., Neal, A.L., Kukkadapu, R.K., Brewe, D., Coby, A. & Picardal, F.W., 2005. Effects of sediment iron mineral composition on microbially mediated changes in divalent metal speciation: importance of ferrihydrite, *Geochimica et Cosmochimica Acta* **69**(7), 1739–1754.

Cornell, R.M. & Schwertmann, U., 1996. *The Iron Oxides,* VCH, Weinheim, Germany.

De Boer, C.B. & Dekkers, M.J., 1998. Thermomagnetic behaviour of haematite and goethite as a function of grain size in various non-saturating magnetic fields, *Geophys J. Int.,* **133,** 541–552.

De Grave, E. & Vandenberghe, R.E., 1986. ^{57}Fe Mössbauer effect study of well-crystallized goethite (α-FeOOH), *Hyp. Interact.,* **28,** 643–646.

De Grave, E., Barrero, C.A., Vandenberghe, R.E., Da Costa, G.M. & Van San, E., 2002. Mössbauer spectra of α- and γ-polymorphs of FeOOH and Fe_2O_3: effects of poor crystallinity and of Al-for-Fe substitution, *Clay Minerals,* **37,** 591–606.

Dekkers, M.J., 1989a. Magnetic properties of natural goethite—I. Grain-size dependence of some low- and high-field related rockmagnetic parameters measured at room temperature, *Geophys. J.,* **97,** 323–340.

Dekkers, M.J., 1989b. Magnetic properties of natural goethite—II. TRM behaviour during thermal and alternating field demagnetization and low-temperature treatment, *Geophys. J.,* **97,** 341–355.

Forsyth, J.B., Hedley, I.G. & Johnson, C.E., 1968. The magnetic structure and hyperfine field of goethite (α-FeOOH), *J. Phys. C (Proc. Phys. Soc. London),* **1,** 179–188.

Guyodo, Y., Mostrom, A., Penn, R. Lee & Banerjee, Subir K., 2003. From nanodots to nanorods: oriented aggregation and magnetic evolution of nanocrystalline goethite, *Geophys. Res. Lett.,* **30**(10), 1512, doi:1029/2003GL017021.

Hedley, I.G., 1971. The weak ferromagnetism of goethite (α-FeOOH), *Zeitschrift fur Geophysik,* **37,** 409–420.

Kilcoyne, S.H. & Ritter, C., 1997. The influence of Al on the magnetic properties of synthetic goethite, *Physica B: Condensed Matter.,* **234–236,** 620–621.

Lee, J.Y., Sei, J., Oh, Sohn, J.G. & Kwon, Soon-Ju, 2001. On the correlation between the hyperfine field and the particle size of fine goethite synthesized in chloride solution, *Corrosion. Sci.,* **43,** 803–808.

Lemaire, B.J., Davidson, P., Ferré, J., Jamet, J.P., Panine, P., Dozov, I. & Jolivet, J.P., 2002. Outstanding magnetic properties of nematic suspensions of goethite (α-FeOOH) nanorods, *Phys. Rev. Lett.,* **88,** 125507(1)–125507(4).

Maher, B.A. & Dennis, P.F., 2001. Evidence against dust-mediated control of glacial-interglacial changes in atmospheric CO_2, *Nature,* **411,** 176–180.

Morup, S., Madsen, M.B., Franck, J., Villadsen, J. & Koch, C.J.W., 1983. A new interpretattion of Mössbauer spectra of microcrystalline goethite: 'superferromagnetism' or 'super-spin glass' behaviour?, *J. Magn. Magn. Mat.,* **40,** 163–174.

Murad, E., 1996. Magnetic properties of microcrystalline iron (III) oxides and related materials as reflected in their Mössbauer spectra, *Phys. Chem. Mineral.,* **23,** 248–262.

Néel, L., 1962. Propriétés magnétiques des grains fins antiferromagnétiques: superparamagnétisme et superantiferromagnétisme, *J. Phys.,* **17,** Suppl. B-1, 676–685.

Nuñez, N.O., Morales, M.P., Tartaj, P. & Serna, C.J., 2000. Preparation of high acicular and uniform goethite particles by a modified-carbonate route, *J. Mater. Chem.,* **10,** 2561–2565.

Özdemir, Ö. & Dunlop, D.J., 1996. Thermoremanence and Néel temperature of goethite, *Geophys. Res. Lett.,* **23**(9), 921–924.

Özdemir, Ö. & Dunlop, D.J., 2000. Intermediate magnetite formation during dehydration of goethite, *Earth planet. Sci. Lett.,* **177,** 59–67.

Pollard, R.J., Pankhurst, Q.A. & Zientek, P., 1991. Magnetism in aluminous goethite, *Phys. Chem. Minerals,* **18,** 259–264.

Rochette, P. & Fillion, G., 1989. Field and temperature behavior of remanence in synthetic goethite: paleomagnetic implications. *Geophys. Res. Lett.,* **16,** 851–854.

Schulze, D.G. & Schwertmann, U., 1984. The influence of aluminium on iron oxides. X. The properties of Al-substituted goethites, *Clay Minerals,* **19,** 521–539.

Schwertmann, U. & Cornell, R.M., 1991. *Iron Oxides in the Laboratory,* VCH publishers, New York, USA.

Schwertmann, U., Cambier, P. & Murad, E., 1985. Properties of goethite of varying crystallinity, *Clays and Clays Minerals,* **33**(5), 369–378.

Strangway, D.W., Honea, R.M., McMahon, B.E. & Larson, E.E., 1968. The magnetic properties of naturally occurring goethite, *Geophys. J. R. astr. Soc.,* **15,** 345–359.

Van der Woude, F. & Dekker, A.J., 1966. Mössbauer effect in α-FeOOH, *Phys. Stat. Sol,* **13,** 181–193.

Wolska, E. & Schwertmann, U., 1993, The mechanism of solid solution formation between goethite and diaspore, *N. Jb. Miner. Mh.,* **5,** 213–223.

Yamamoto, A., Honmyo, T., Hosoito, N., Kiyama, M. & Shinjo, T., 1993. Surface magnetism of α-FeOOH by Mössbauer spectroscopy, *Nucl. Instrum. &Methods in Phys. Res.,* **B76,** 202–203.